EDF
Electricité de France

Direction des Etudes et Recherches

SERVICE RÉACTEURS NUCLÉAIRES ET ECHANGEURS
Département Mécanique et Technologie des Composants
Département Etude des Matériaux

1993

MOINEREAU D.
ROUSSELIER G.
BETHMONT M.

COMPORTEMENT DES DEFAUTS SOUS REVETEMENT DANS LES CUVES REP - EVALUATION DES METHODES D'ANALYSE A PARTIR D'ESSAIS DE MAQUETTES REVETUES

BEHAVIOR OF UNDERCLAD CRACKS IN REACTOR PRESSURE VESSELS - EVALUATION OF MECHANICAL ANALYSES WITH TESTS ON CLADDED MOCK-UPS

Pages : 00016

94NB00136

Diffusion : J.-M. Lecœuvre
EDF-DER
Service IPN. Département SID
1, avenue du Général-de-Gaulle
92141 Clamart Cedex

ISSN 1161-0611

SYNTHÈSE :

La nocivité des défauts sous revêtement susceptibles d'exister dans les cuves des réacteurs REP doit être examinée vis-à-vis du risque de rupture brutale, en particulier en fin de durée de vie des cuves en raison de la fragilisation du matériau qui la constitue. Cette nocivité est évaluée à partir d'analyses mécaniques élastique ou élastoplatique prenant en compte notamment la présence du revêtement inoxydable. EDF a engagé un programme d'étude comportant des essais sur des maquettes de grandes dimensions et les interprétations correspondantes. Ce programme est destiné à évaluer les différentes méthodes d'analyse mécanique susceptibles d'être mises en œuvre dans les études de sûreté.

Plusieurs maquettes en acier ferritique A508 C13 revêtu d'acier inoxydable et comportant des petits défauts situés sous le revêtement sont testées en flexion 4 points. Les essais sont effectués à très basse température pour simuler la fragilisation du métal de base par l'irradiation et obtenir une instabilité des défauts par clivage.

Trois essais ont été réalisés sur des maquettes comportant un petit défaut sous revêtement (d'une profondeur d'environ 5 mm) et un quatrième essai a été effectué sur une maquette présentant une fissure plus profonde (environ 13 mm). Dans chaque cas, l'instabilité de la fissure est obtenue par clivage dans le métal de base à température d'environ - 170 °C, sans arrêt de la propagation.

Chaque essai est interprété par des analyses élastiques et élastoplastiques au moyen de calculs aux éléments finis bidimensionnels. Les ruptures sont correctement prédites : les facteurs d'intensité de contrainte (K_{cp} ou K_J) sont toujours supérieurs à la ténacité du métal de base. Les analyses élastiques (comprenant deux corrections de plasticité) sont généralement conservatives par rapport aux analyses élastoplastiques. L'effet favorable du revêtement apparaît également.

EXECUTIVE SUMMARY :

Innocuity of underclad flaws in the reactor pressure vessels must be demonstrated in the French safety analyses, particularly in the case of a severe transient at the end of the pressure vessel lifetime, because of the radiation embrittlement of the vessel material. Safety analyses are usually performed with elastic and elasto-plastic analyses taking into account the effect of the stainless steel cladding. EDF has started a program including experiments on large size cladded specimens and their interpretations. The purpose of this program is to evaluate the different methods of fracture analysis used in safety studies.

Several specimens made of ferritic steel A508 C1 3 with stainless steel cladding, containing small artificial defects, are loaded in four-point bending. Experiments are performed at very low temperature to simulate radiation embrittlement and to obtain crack instability by cleavage fracture.

Three tests have been performed on mock-ups containing a small underclad crack (with depth about 5 mn) and a fourth test has been performed on one mock-up with a larger crack (depth about 13 mn). In each case, crack instability occured by cleavage fracture in the base metal, without crack arrest, at a temperature of about - 170°C.

Each test is interpreted using linear elastic analysis and elastic-plastic analysis by two-dimensional finite element computations. The fractures are conservatively predicted : the stress intensity factors deduced from the computations (K_{cp} or K_J) are always greater than the base metal toughness. The comparison between the elastic analyses (including two plasticity corrections) and the elastic-plastic analyses shows that the elastic analyses are often conservative.

The beneficial effect of the cladding in the analyses is also shown : the analyses are too conservative if the cladding effect is not taken into account.

BEHAVIOR OF UNDERCLAD CRACKS IN REACTOR PRESSURE VESSELS. EVALUATION OF MECHANICAL ANALYSES USED IN FRENCH RPV INTEGRITY ASSESSMENT BY CLEAVAGE FRACTURE TESTS ON LARGE SCALE PLATES.

D. MOINEREAU, G. ROUSSELIER, M. BETHMONT

ELECTRICITE DE FRANCE
Service Réacteurs Nucléaires et Echangeurs
77250 Moret-sur-Loing, FRANCE

1- INTRODUCTION

Innocuity of underclad flaws in the reactor pressure vessels must be demonstrated in the French safety analyses, particularly in case of severe overcooling transient at the end of their lifetime because of the radiation embrittlement of the vessel material. These safety analyses are usually performed with elastic and elasto-plastic analyses taking into account the effect of the stainless steel cladding. EDF has started a program including experiments on large size cladded specimens and their interpretations by fracture mechanics. The purpose of this program is to evaluate the different methods of fracture analysis used in these safety studies.
Several specimens made of ferritic steel A508 Cl 3 with stainless steel cladding, containing small artificial defects, have been loaded in four-point bending. Experimentations are performed at very low temperature to simulate radiation embrittlement and to obtain crack instability by cleavage fracture.
Four tests have been performed on mock-ups containing an underclad crack. In each case, the crack instability has been obtained by cleavage fracture in base metal, without crack arrest, at a temperature of abont -170°C.
This paper describes the experimental program with the main results and presents the mechanical analyses of each test using elastic and elastic-plastic fracture mechanics.

2- THE EXPERIMENTAL PROGRAMME

2.1 Mock-ups

Four mock-ups (DSR4, DSR1, DSR3, DD2), each containing an underclad crack, have been submitted to a mechanical loading. The mock-ups geometry is a four-point bend bar specimen (figure 1). The central part of each mock-up is extracted from a vessel shell ring of A508 Cl3 ferritic steel. The size of the specimens is approximately 120 mm thickness, 1700 mm length and 150 mm width. The cladding is layered on the top surface using an automatic submerged-arc welding process. After cladding, a stress relief heat treatment is applied at 600°C for 8 hours. The artificial underclad crack is made before cladding by machining and fatigue. An ultrasonic examination is performed on each mock-up after manufacturing to determine the crack depth.

2.2 Testing conditions

The specimens are loaded in four-point bending, as shown in figure 1 with a 1450 mm major span and 450 mm minor span (except in the DSR4 test where the minor span is 250 mm). Each test has been performed at low temperature (about -170°C) to obtain crack instability in base metal by cleavage fracture and to have base metal toughness representative of the vessel material toughness at the end of life. The mock-ups are instrumented with thermocouples (placed on surface and inside the specimen) to control the temperature during the test (each mock-up is insulated to avoid significant reheating during the experiment).

2.3 Materials characterization

Characterization of stainless steel cladding, base metal and heat-affected zone has been performed including chemical analyses, Charpy impact tests, tensile tests, crack-growth resistance and fracture toughness. The chemical composition of the base metal is given in table 1. The base metal toughness K_{1C}, measured on 20% side grooved CTJ25 specimens (net thickness 20 mm), is presented in figure 2 (RTNDT = - 40°C).

2.4 Experimental results

The cleavage fracture has been obtained on the four mock-ups without crack arrest. The fracture surface of each

mock-up is presented on the figure 3 : the surface aspect is typical of a cleavage fracture, at least in the upper part of the section. The cracks shape is practically semi-elliptical :

- DSR4 test
The mock-up fracture is reached with a load of 640 kN.
The crack size is 5 mm deep and 50 mm wide. The cladding thickness is 8 mm and the mock-up is 145 mm wide.

- DSR1 test
The mock-up fracture is reached with a load of 804 kN.
The crack size is 4 mm deep and 50 mm wide. The cladding thickness is 5 mm and the mock-up is 150 mm wide.

- DSR3 test
The mock-up fracture is reached with a load of 695 kN.
The crack size is 13 mm deep and 40 mm wide.The cladding thickness is 4.5 mm and the mock-up is 150 mm wide.

- DD2 test
The mock-up fracture is reached with a load of 890 kN.
Crack size is 4.5 mm deep and 50 mm wide. The cladding thickness is 6 mm and the mock-up is 150 mm wide.

3- MECHANICAL ANALYSES METHODS

The four tests are interpreted with linear elastic analyses and elastic-plastic analyses including two-dimensional (DSR4, DSR1, DSR3, DD2 mock-ups) and three-dimensional (DSR4, DSR3 mock-ups) finite element computations.
The analyses are performed both with and without residual stresses taken into account. The stress intensity factors calculated in these different analyses are compared to the base metal toughness K_{1C}.

3.1 Two-dimensional elastic and elastic-plastic analyses

The stress intensity factors K_I or K_J are calculated with the finite element program SYSWELD.

In the elastic analyses, after the computation of K_I, two corrections are applied to take into account plasticity at the crack tips (Irwin correction) and in the cladding (α correction), according to the approach proposed for the analysis of the French PWR vessels (1)(2)(3) :

Irwin correction :

$$K_{irwin} = K_I \cdot \sqrt{\frac{2a + r_a + r_b}{2a}}$$

with $2a$: crack depth
r_a, r_b : plastic zone radius at the crack tip in cladding and base metal given by

$$r = \frac{1}{6\Pi}\left(\frac{K_I}{\sigma_y}\right)^2$$

σ_y is the yield strength of the corresponding material

α correction :

$$K_{cp} = \alpha . K_I . \sqrt{\frac{2a + r_a + r_b}{2a}}$$

α is a coefficient depending on the plastic zone radius and the remaining ligament value b between the crack tip and the surface. This coefficient is determined by :

$\alpha = 1$ if $r < 0.05b$

$$\alpha = 1 + 0.15\left(\frac{r - 0.05\,b}{0.035\,b}\right)^2$$

if $0.05b < r < 0.085b$

When the condition $r = 0.085\ b$ is exceeded, α is the lowest of the value given by the above expression and the limiting value 1.6

In the elastic-plastic analyses, the stress intensity factors K_J are deduced from the calculation of the J integral. The integral J is calculated on several paths to verify path independancy.

3.2 Residual stresses

Because of the difference in thermal expansion coefficients between the cladding and the base metal, residual

stresses develop in the mock-ups due to the cooling from the stress relief heat treatment temperature to the test temperature (about -170°C). Residual stresses related to metallurgical transformations are not considered here.
In the elastic analyses, those stresses are coarsely simulated. The stress intensity factor K_{res} due to residual stresses is calculated by using the simplified model described in figure 4 (4). Magnitude of residual stresses is obtained by the elastic-plastic simulation of the cooling process after the stress relief heat treatment ; the specimen is assumed to be stress free at the stress relief anneal temperature (600°C) and the temperature distribution inside the specimen is assumed to be uniform at all times during the controled cooling to the test temperature. Then, the stress intensity factor K_{res} is added to the S.I.F. $K_{loading}$ due to the mechanical loading : $K_I = K_{res} + K_{loading}$. The final S.I.F. K_{cp} is obained by applying the two plasticity corrections described in 3.1 (Irwin correction, α correction).
In the elastic-plastic analyses, the residual stresses are taken into account by simulating in the first step of the calculation (before the mechanical loading) the cooling process. The S.I.F. K_J is deduced from the calculation of the J integral.

3.3 Three-dimensional elastic and non linear elastic analyses

The three-dimensional analyses are performed with the finite element program PERMAS. The stress intensity factors (linear elastic or non linear-elastic) are calculated along the crack front by the mean of the energy release rate G. G is obtained by the Theta method described in (5)(6). Residual stresses are not taken into account.

3.4 Simplified analysis without taking into account the cladding

In this case, we assume that the crack is a semi-elliptical surface crack. The cladding is not taken into account. The stress intensity factor along the surface crack front is obtained by formulae proposed by Newman-Raju (7). Residual stresses are not taken into account.

4- INTERPRETATION OF TESTS

4.1 Interpretation of tests without taking into account the cladding

The maximum value of the stress intensity factor K_I in base metal, calculated by Newman-Raju formulae, is obtained for the four tests at the deepest point of the crack. The stress intensity factors K_I obtained for each critical load (tables 2, 3, 4 and 5) are compared to the base metal toughness K_{IC} in figure 5. Those values are clearly greater than the base metal toughness.

4.2 Interpretation of tests with elastic analyses without residual stresses

The stress intensity factors K_I (before plasticity corrections) and K_{cp} (after the two plasticity corrections) obtained on each mock-up at the fracture are presented in the tables 2, 3, 4, 5. These S.I.F. are compared to the base metal toughness K_{IC} in figure 6. These values are also greater than the base metal toughness : the margins are important as soon as the α correction is significant (case of DSR1, DSR3 and DD2 tests). The two-dimensional analysis of DSR3 test (crack depth : 13 mm) appears too conservative compared to the three-dimensional analysis (see the values of K_I in table 4).

4.3 Interpretation of tests with elastic-plastic analyses without residual stresses

The stress intensity factors K_J obtained on each mock-up at the fracture are presented in the tables 2, 3, 4 and 5. The comparison with the base metal toughness K_{IC} shows reasonable margins

(figure 7). These margins are smaller than in the elastic analyses except for the DSR4 test for which the α correction is not significant ($\alpha < 1.1$).

4.4 Interpretation of tests with residual stresses

In the elastic analyses, the magnitude of residual stresses is obtained by the elastic-plastic simulation of the cooling process after the stress relief heat treatment as described previously. This simulation gives for all mock-ups tensile stresses in the cladding and low compressive stresses in the heat-affected zone of base metal. The magnitude of those residual stresses is about + 160 MPa in the cladding and between - 30 and -45 MPa in the base metal (according to the mock-ups). These values are similar to experimental values measured on cladded mock-ups (EDF mock-up, and (8)). The stress intensity factors are calculated by taking into account or not the low compressive stresses in the base metal (in this last case, $\sigma_{res\text{-}clad}$ = 160 MPa and $\sigma_{res\text{-}bm}$ = 0 MPa).

The stress intensity factors in base metal K_{cp}, K_J calculated by taking into account residual stresses are presented in tables 2 (DSR4 test); 3 (DSR1 test), 4 (DSR3 test) and 5 (DD2 test). Main results of DSR4, DSR1 and DD2 tests are gathered in table 6.
These results show an increase of the stress intensity factor K_J in base metal in the elastic-plastic analyses when residual stresses are taken into account in spite of low compressive residual stresses in the heat-affected zone. It is a consequence of the more important plastification of the cladding due to tensile residual stresses.

In the elastic analyses (including the plasticity corrections), the stress intensity factor K_{cp} in base metal increases with residual stresses if we consider only the tensile residual stresses ($\sigma_{res\text{-}clad}$ = 160 MPa and $\sigma_{res\text{-}bm}$ = 0 MPa in the simplified model described previously). It is not always the case if we consider also the low compressive residual stresses in the base metal.
The values of the stress intensity factors K_{cp}, K_J at the upper crack tip (cladding side) are not presented in this paper. K_{cp} and K_J always increase when residual stresses are taken into account ; this increase is more important than in the base metal (about 20 % in the cladding).

5- DISCUSSION

The comparison between those different results shows that a simplified mechanical analysis which doesn't take into account the cladding (a small underclad crack is assumed to be a semi-elliptical surface crack) is too conservative. Taking into account the mechanical effect of the cladding decreases the stress intensity factor at the crack tip in base metal with however suffisant margins.
The comparison between the elastic analyses and the elastic-plastic analyses (with residual stresses or not) shows that the elastic analyses are conservative as soon as the plastic deformation in the cladding is not negligible. This conservatism seems to be due to the α correction proposed in the French RCC-M code which takes into account the plastification in the cladding. This correction is important as soon as the plastic zone at the cladding side crack tip reaches a notable proportion of the remaining ligament. This correction is however necessary because an elastic analysis can greatly underestimate the crack opening in base metal when plastic straining of the cladding occurs (figure 8).

How to explain the observed margins when comparing the stress intensity factors in base metal to the base metal toughness K_{1C} ?. Several assumptions can be suggested :

. The toughness K_{1C} curve used in the

comparison is the base metal toughness curve and not the heat-affected zone toughness curve. The characterization of the H.A.Z. is in progress.

. In this program, the underclad cracks have generally a small depth (4 to 5 mm in DSR4, DSR1, DD2 mock-ups) and the ratio a/w (crack depth compared to base metal thickness) is small (about 0.05). The base metal toughness K_{IC} has been determined on small CT25 specimens for which the ratio a/w is higher (a/w = 0.55). Is there a "shallow crack" effect ?. The work of T.J. THEISS and S.T. ROLFE (9) suggests a shallow flaw fracture toughness enhancement under these conditions.

. In the case of small underclad cracks, two-dimensional and three-dimensional calculations give similar values of the stress intensity factor at the crack tip in base metal (5) and it is the maximum value of the stress intensity factor which is compared to the toughness K_{IC}. The three-dimensional calculations performed in this programme (5) show that the S.I.F. is not constant along the crack-front in base metal (figure 9). The use of the maximum value of the S.I.F. in the comparison with the toughness K_{IC} is perhaps too severe : the use of an average value of the S.I.F. along the crack-front could be more realistic and so less conservative as suggested in the study (10).

. The classical analyses for cleavage fracture (elastic or elastic-plastic by the mean of the stress intensity factor) do not take into account the size effect (crack width) in cleavage fracture. This effect could be taken into account with the local approach of cleavage fracture (2). The interpretation of the tests with this approach is in progress.

6- CONCLUSION

EDF is carrying out an experimental and numerical study in order to evaluate different methods of fast fracture analysis which are used in the reactor pressure vessel integrity assessments.

Four mechanical tests have been performed in four-point bending on large size mock-ups containing an underclad crack made by fatigue before cladding. A cleavage fracture initiated in base metal has been obtained on each mock-up at a temperature of about - 170°C.

The cleavage fracture of each mock-up are always conservatively predicted by an elastic analysis including plasticity corrections (Irwin correction and α correction) . and by an elastic-plastic analysis : the stress intensity factors K_{cp} or K_J are always greater than the base metal toughness K_{IC}. The comparison between the elastic analysis and the elastic-plastic analysis shows that the first one is often more conservative ; it is due to the fact that the α correction proposed in French RCC-M code is important as soon as the plastic zone at the crack tip reaches a notable proportion of the remaining ligament. However, the comparison between K_{cp} (elastic analysis) and K_J (elastic-plastic analysis) shows that the α correction is necessary because the elastic analysis underestimates the crack opening in base metal when plastic deformation of the cladding occurs.

The effect of the residual stresses has been also examined : the stress intensity factor K_J in base metal increases in the elastic-plastic analyses when residual stresses are taken into account in spite of low compressive residual stresses in the heat-affected zone. This is a consequence of the more important plastic deformation of the cladding due to tensile residual stresses.

The favourable effect of the cladding is also shown : a simplified mechanical analysis in which the cladding is not taken into account (by assuming that the crack is a semi-elliptical surface crack) appears to be too conservative.

New tests are in progress involving cladded specimens containing a small crack in the first layer of cladding. The conservatism of the analyses proposed by the RCC-M code will be evalnated for this

crack configuration. The conservatism of the plasticity corrections defined in RCC-M code will be also examined in case of a thermal loading (as an overcooling transient). Thermal shock tests on a cladded vessel could be considered.

ACKNOWLEDGEMENTS

The authors thank Mr FAIDY, Mr RIEG and Mrs CHURIER-BOSSENNEC from Electricité de France (SEPTEN) for their cooperation and support for this study.

REFERENCES

(1) RCC-M , January 1988 Edition "Design and Construction rules for mechanical components of PWR nuclear islands - RCC-M - AFCEN France"

(2) A. PELLISSIER-TANON, J. GRANDEMANGE, B. HOUSSIN, C. BUCHALET "French experience on the verification of pressurized water reactor vessels integrity", EPRI Research projet 2975-2, 1989

(3) A. PELLISSIER-TANON, S. BHANDARI, J. VAGNER "Practical methods for surface and sub-surface cracks in reactor pressure vessels", ASME PRESSURE VESSELS AND PIPING CONFERENCE, San Diego, 1991

(4) J.L. BERNARD, J. VAGNER, A. PELLISSIER-TANON, F. FAURE "Effect of residual stresses and complex loadings on the fatigue behavior of underclad cracks", SMIRT 9, Lausanne, 1987

(5) G. DEBRUYNE, D. MOINEREAU "Crack analysis of cladded mock-ups in the frame of brittle and ductile fracture", SMIRT 11, Tokyo, 1991

(6) Y. WADIER, O. MALAK "The Theta method applied to the analysis of 3D elastic-plastic cracked bodies", SMIRT 10, Anaheim, 1989

(7) J.C. NEWMAN, I.S. RAJU "An empirical stress-intensity factor equation for the surface crack" - Engineering Fracture Mechanics - vol 15, n°1-2, pp 185-192, 1981

(8) H.A. SCHIMMOELLER, J.L. RUGE "Estimation of residual stresses in reactor pressure vessel steel specimens clad by stainless steel strip electrodes", International Conference on Residual Stresses in welded construction and their effects, London, 1977

(9) T.J. THEISS, S.T. ROLFE, D.K. SHUM "Shallow-crack toughness results for reactor pressure vessel steel", International Conference Shallow Crack Fracture Mechanics, Toughness Tests and Applications, Cambridge, 1992

(10) M. BEGHINI, L. BERTINI, E. VITALE "Three dimensional interpretation of crack initiation during thermal shock loading of thick plates", ASME PRESSURE VESSELS AND PIPING CONFERENCE, New Orleans, 1992

TABLE 1 – CHEMICAL COMPOSITION OF THE FERRITIC STEEL A503 C13 (weight %)

	C	S	P	Mn	Si	Ni	Cr	Mo	V	Cu	Co	Al
RCC-M specification	⩽0.22	⩽0.008	⩽0.008	1.15 1.60	0.10 0.30	0.50 0.80	⩽0.25	0.43 0.57	⩽0.01	⩽0.08	⩽0.03	⩽0.04
Inner surface	0.14	0.004	0.006	1.31	0.19	0.72	0.17	0.51	<0.01	0.07	<0.01	0.015
1/4 thickness	0.18	0.004	0.006	1.32	0.19	0.73	0.17	0.51	<0.01	0.07	⩽0.01	0.016

TABLE 2 – INTERPRETATION OF DSR4 TEST

analysis	K_I MPa.m^0.5	α correction	K_{cp} MPa.m^0.5	K_J MPa.m^0.5
2D elastic without residual stresses	38.0	1.012	40.5	
2D elastic with tensile-compressive residual stresses	34	1.04	36.4	
2D elastic with tensile residual stresses	38.1	1.07	43.0	
2D elastic-plastic without residual stresses				44.5
2D elastic-plastic with residual stresses				50.0
3D simplified analysis (surface crack)	67.9		70.5	

TABLE 3 – INTERPRETATION OF DSR1 TEST

analysis	K_I MPa.m^0.5	α correction	K_{cp} MPa.m^0.5	K_J MPa.m^0.5
2D elastic without residual stresses	41.3	1.43	63.6	
2D elastic with tensile-compressive residual stresses	38.9	1.58	66.3	
2D elastic with tensile residual stresses	41.4	1.6	72.2	
2D elastic-plastic without residual stresses				52.0
2D elastic-plastic with residual stresses				58.8
3D simplified analysis (surface crack)	67.1		70.4	

TABLE 4 – INTERPRETATION OF DSR3 test

analysis	K_I MPa.m^0.5	α correction	K_{cp} MPa.m^0.5	K_J MPa.m^0.5
2D elastic without residual stresses	61.0	1.6	105.5	
2D elastic with tensile residual stresses	61.1	1.6	106.4	
2D elastic-plastic without residual stresses				79.3
3D elastic without residual stresses	48.0			
3D non linear elastic without residual stresses				53.0
3D simplified analysis (surface crack)	71.3		74.8	

TABLE 5 – INTERPRETATION OF DD2 TEST

analysis	K_I MPa.m^0.5	α correction	K_{cp} MPa.m^0.5	K_J MPa.m^0.5
2D elastic without residual stresses	46.9	1.54	78.5	
2D elastic with tensile-compressive residual stresses	44.0	1.6	76.9	
2D elastic with tensile residual stresses	47.0	1.6	82.8	
2D elastic-plastic without residual stresses				61.5
2D elastic-plastic with residual stresses				68.7
3D simplified analysis (surface crack)	78.4		83	

TABLE 6 – EFFECT OF RESIDUAL STRESSES IN DSR4, DSR1 AND DD2 TESTS

analysis	stress intensity factor	DSR4 test	DSR1 test	DD2 test
2D elastic without residual stresses	K_{cp}	40.5	63.6	78.5
2D elastic with tensile-compressive residual stresses	K_{cp}	36.4	66.3	76.9
2D elastic with tensile residual stresses	K_{cp}	43.0	72.2	82.8
2D elastic-plastic without residual stresses	K_J	44.5	52	61.5
2D elastic-plastic with residual stresses	K_J	50	58.8	68.7

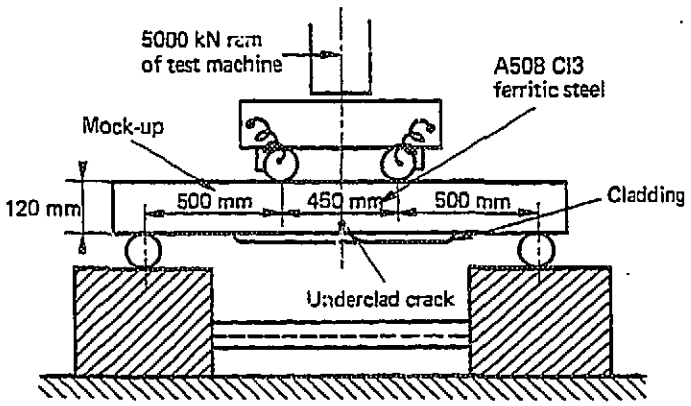

Figure 1 — Schematic of the test frame used in four-point bending fracture experiments.

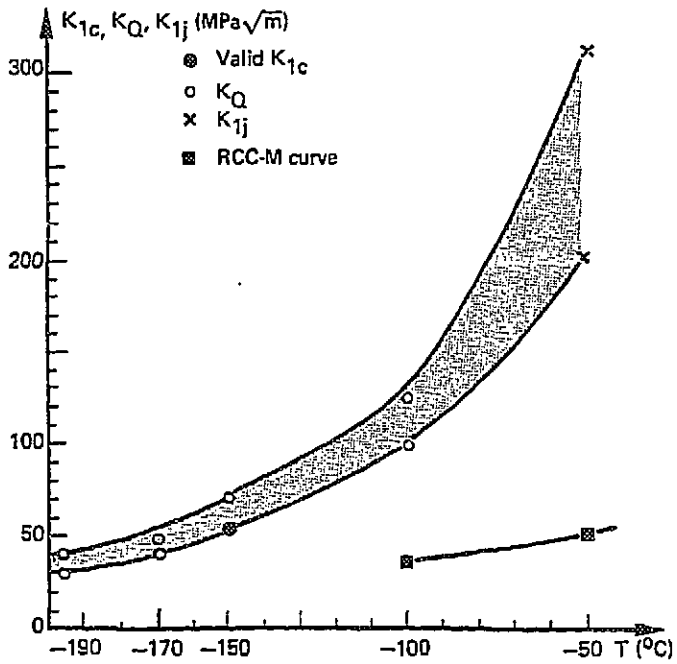

Figure 2 — Toughness of base metal (CTJ25 specimens). RTNDT = −40°C.

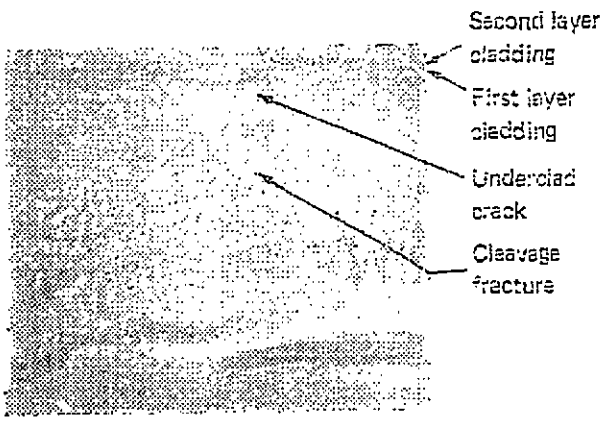

Cross-section of DSR4 mock-up after fracture

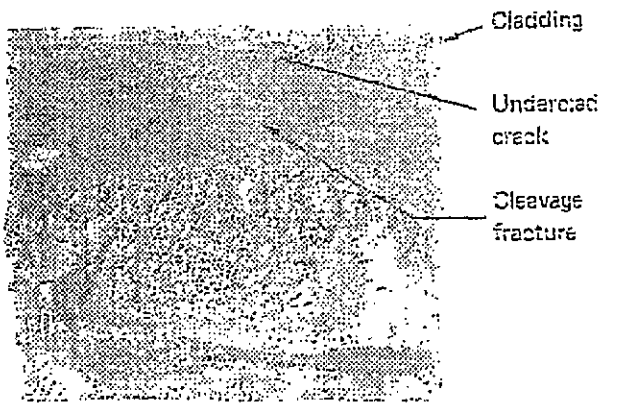

Cross-section of DSR1 mock-up after fracture

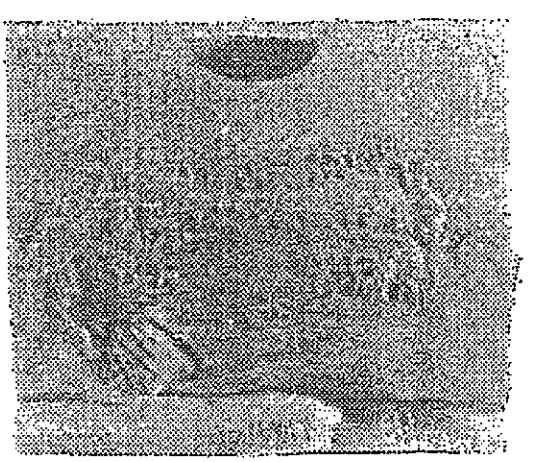

Cross-section of DSR3 mock-up after fracture

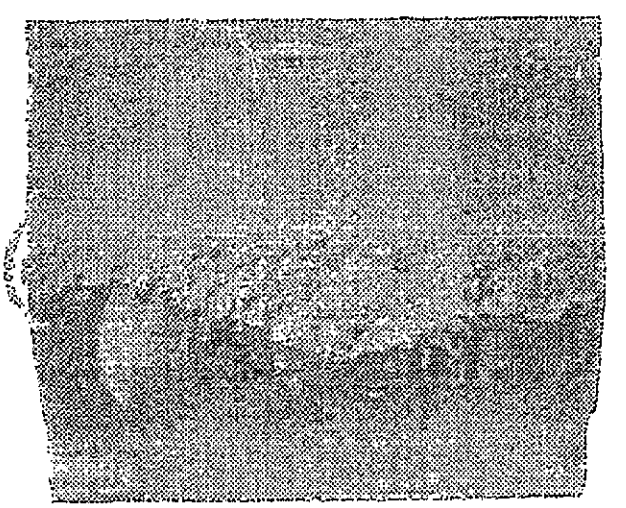

Cross-section of DD2 mock-up after fracture

Figure 3 — Cross-section of mock-ups after fracture.

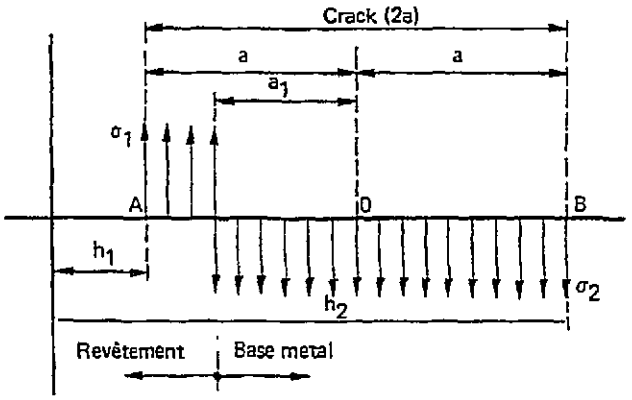

$$K_{iA} = F_A\sqrt{\pi a}\,[\sigma_1 + \alpha_A\,(\sigma_2 - \sigma_1)]$$

$$K_{iB} = F_B\sqrt{\pi a}\,[\sigma_1 + \alpha_B\,(\sigma_2 - \sigma_1)]$$

$$\alpha_A = \frac{\pi/2 - \emptyset 1 - \cos \emptyset 1}{\pi}$$

$$\alpha_B = \frac{\pi/2 - \emptyset 1 + \cos \emptyset 1}{\pi}$$

$$\emptyset 1 = \text{Arc sin } \frac{a_1}{a}$$

Figure 4 – Model for the stress intensity factors determination in a two levels residual stress field (4).

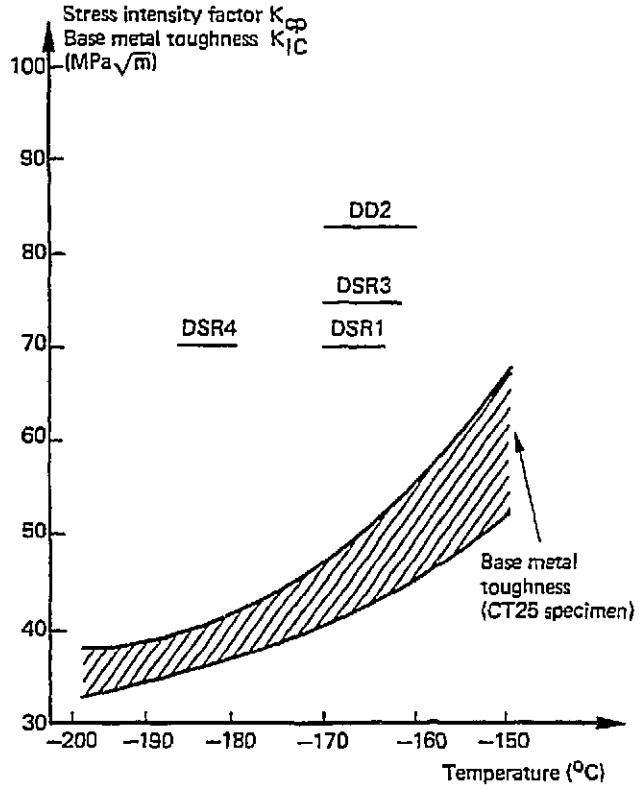

Figure 5 – Interpretation of tests without taking into account the cladding.

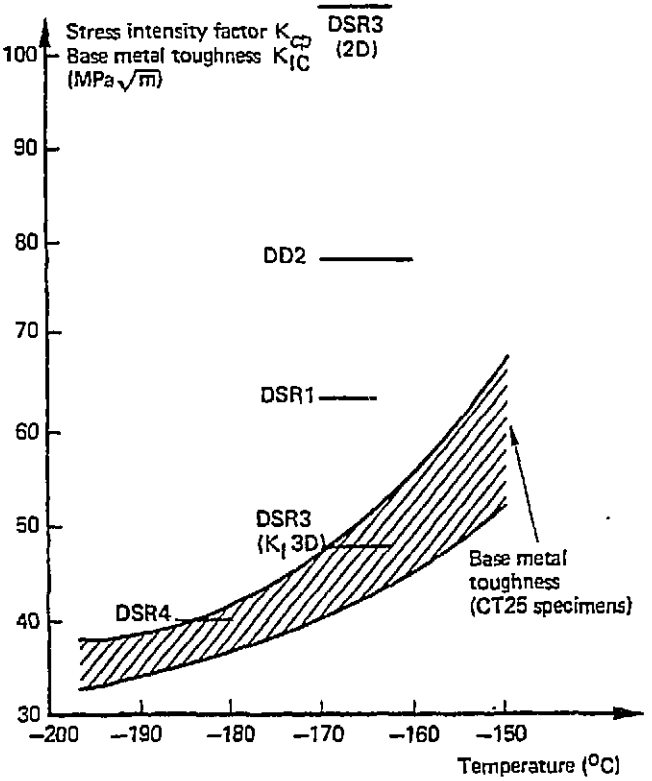

Figure 6 – Interpretation of tests with elastic analyses.

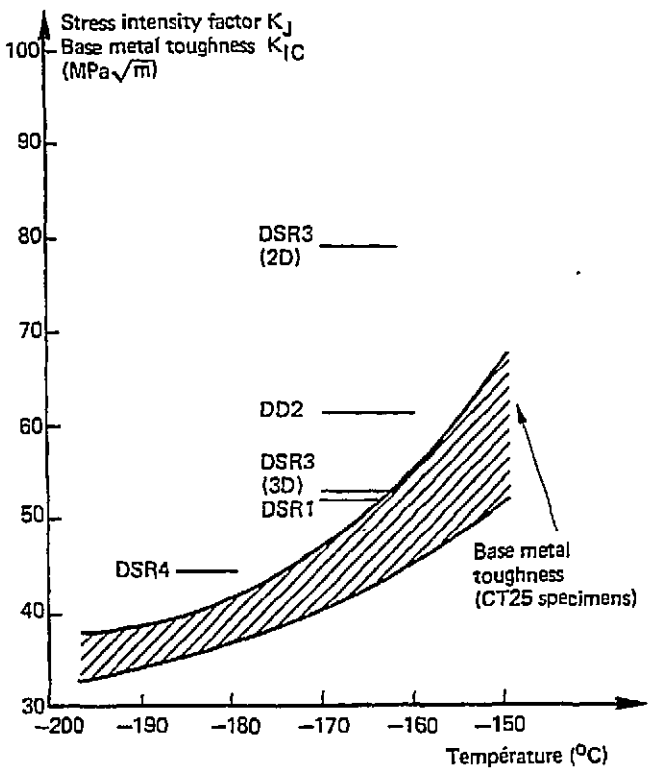

Figure 7 – Interpretation of tests with elastic-plastic analyses.

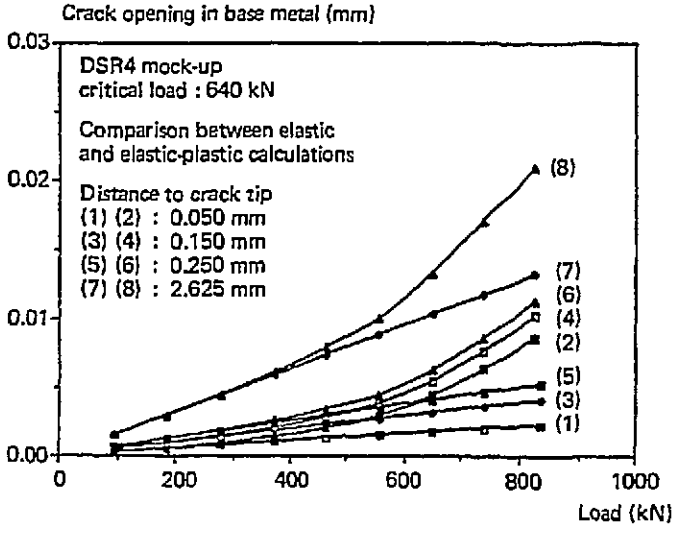

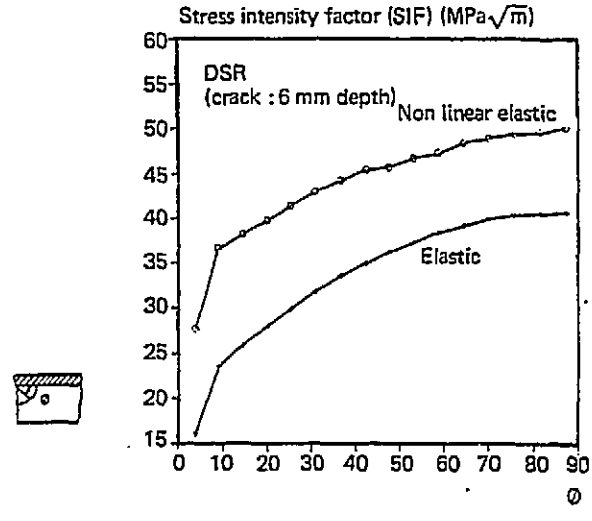

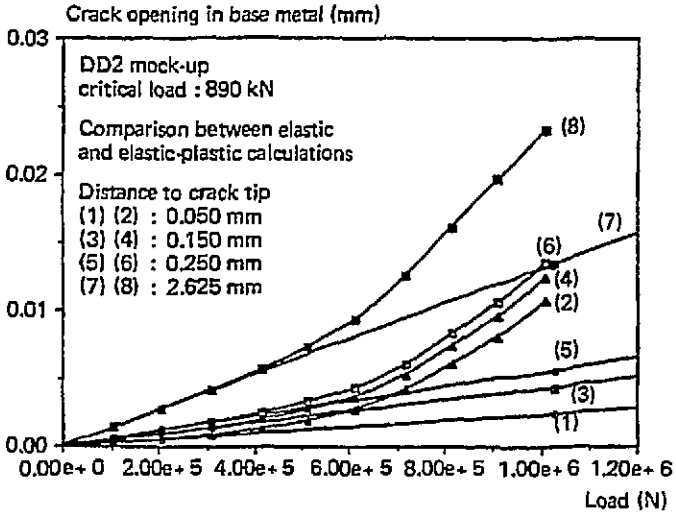

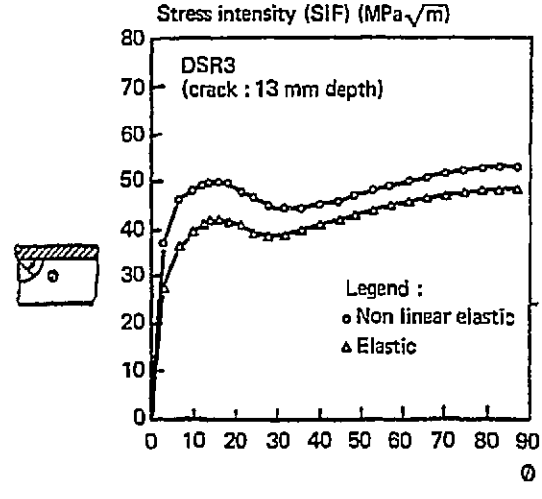

Figure 8 — Crack opening in base metal for DSR4 and DD2 mock-ups. Comparison between elastic and elastic-plastic calculations.

Figure 9 — Three dimensional analyses of tests. Evolution of K_I along the crack-front in base metal.

EDF
Electricité de France

Direction des Etudes et Recherches

Service Information Prospective et Normalisation

Département Systèmes d'information et de documentation

Groupe Exploitation de la Documentation Automatisée

1, avenue du Gal de Gaulle
92141 CLAMART Cedex
tel : 47 65 56 33

CLAMART Le 02/06/95

CEA
MIST/SBDS/SPRI
CENTRE DE SACLAY

91191 GIF SUR YVETTE CEDEX

à l'attention de :

MEMOIRE TECHNIQUE ELECTRONIQUE

****
Cette feuille est détachable grâce à la microperforation sur le coté droit.
****

Référence de la demande : **F528203** Votre commande :
Origine : **CATALOGUE DES NOTES DER**

Numéro du document : **94NB00136**

Titre : **COMPORTEMENT DES DEFAUTS SOUS REVETEMENT DANS LES CUVES REP - EVALUATION DES METHODES D'ANALYSE A PARTIR D'ESSAIS DE MAQUETTES REVETUES**

Auteurs : **MOINEREAU D./ROUSSELIER G./BETHMONT M.**

Source : **COLL. NOTES INTERNES DER. PRODUCTION D'ENERGIE (HYDRAULIQUE, THE**
Serial :

Référence du document : **SANS**

Nombre de pages: **0016** Nombre d'exemplaires : **001** Support : **P**